 DOI:10.30420/566414062

Model Predictive Current Control for PMSM Drives with Low Parameter-dependent Model

Xiang Yu[1], Xiaoguang Zhang[1], Guofu Zhang[1]

[1]North China University of Technology, China

Corresponding author: Xiaoguang Zhang, zxg@ncut.edu.cn

Poster presentation: Xiang Yu , 2023322070110@mail.ncut.edu.cn

Abstract

In conventional model predictive current control (T-MPCC) method, the motor parameters are subject to perturbation errors due to temperature increase, magnetic saturation, or other nonlinear factors, making the motor parameters inaccurate. Inaccurate motor parameters further lead to inaccurate current prediction models, which adversely affects the motor control effectiveness. In this paper, a low parameter-dependent model control method for PMSM drives is proposed to solve the effects of perturbation errors in motor parameters. The method is suitable for surface-mounted permanent magnet synchronous motor (SPMSM), and the parameter values of the inductance and magnetic flux are extracted from the error between the predicted currents of the q-axis in the ideal condition without parameter perturbation and in the actual operating condition. Then, bring the extracted inductance and magnetic flux parameter into the current prediction model for real-time updating. As verified by simulation, the method can reduce the dependence of the current prediction model parameters, and also can enhance the robustness of the drive system parameters.

1 Introduction

With the development of permanent magnet synchronous motor (PMSM), it has attracted the attention and research of many scholars because of its high-power density, simple structure, easy to control, and flexible rotor shape design. The conventional PMSM control basically adopts the magnetic field-oriented control (FOC) [1] or the control method based on direct torque control (DTC) [2] to obtain high control performance. With the development of electronic technology, a method to realize predictive control based on the mathematical model of control object-Model Predictive Control (MPC) has been proposed. MPC can be divided into Finite Control Set Model Predictive Control (FCS-MPC) and Continuous Control Set Model Predictive Control (CCS-MPC) according to the difference of control sets [3], [4]. In FCS-MPC control method, Model Predictive Current Control (MPCC), and Model Predictive Voltage Control (MPVC) depending on the control object [5]. Among them, the MPCC control method has been intensively studied by many scholars due to its good dynamic performance and fast response to sudden changes in load torque and speed.

Since the MPCC control method depends on an accurate system model for prediction, if the parameters of the system model deviate from the actual values, it will lead to lead to degraded control performance, therefore, the precision of the predictive model parameters is crucial for the MPCC control performance. Aiming at the mismatch problem of the predictive model motor parameters, a simple robust MPC method is proposed in the literature [6], where a separating integral controller is designed to extract the accurate inductance parameter based on the prediction current error. Literature [7] and [8] constructed observers to observe current or voltage disturbances and compensated them in real time. Literature [9] and [10] construct parameter observers to observe the exact parameter values and correct the mismatched parameters in real time. Although the above methods can enhance the robustness of the motor drive system, the process of constructing either the integral controller or the observer is complicated. In this regard, a novel online discrete-time parameter identification algorithm is proposed in the literature [11], which identifies the SPM discrete-time model parameters through the model reference adaptive system technique and Popov's super-stability criterion. Literature [12] proposes an extended Kalman filter based permanent magnetic flux identification method for IPMSM, and adopts Model Reference Adaptive System based rotor magnetic flux vector control as the basic control method for IPMSM drives. Literature [13] presents an online parameter estimation method for internal permanent magnet synchronous motor (IPMSM) based on discrete-time dynamic model for accurate estimation of stator resistance, rotor magnetic chain and load torque. All of the above methods can obtain accurate predictive model parameters, but the computations of the proposed methods are very large, which will increase the running time of the program.

In this paper, a simpler and more reliable MPCC control method is proposed. Firstly, in Section 2, the topology of the PMSM control system and the traditional MPCC control method are briefly introduced.

ISBN 978-3-8007-6414-3

Section 3 focuses on the MPCC method for PMSM driver with low parameter-dependent model proposed in this paper. Then, Section 4 verifies the effectiveness of the proposed method through simulation experiments. Finally, in Section 5, a comprehensive summary of the whole paper is presented.

2 PMSM System Topology and Conventional MPCC Method

2.1 PMSM Control System Topology

PMSM drive control system containing a voltage source inverter(2L-VSI), which topology is shown in Fig. 1:

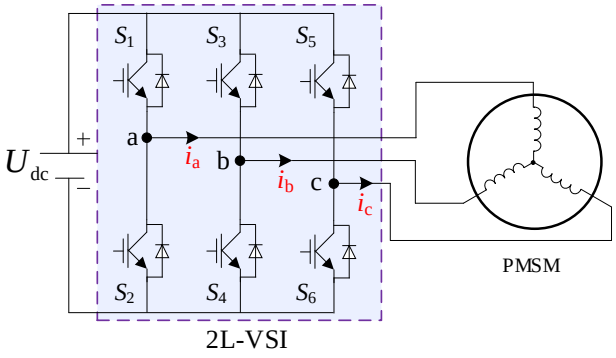

Fig. 1. PMSM control system topology

The mathematical equations for the voltage of PMSM in the d-axis and q-axis are as follows:

$$\begin{cases} u_d = Ri_d - L_q \cdot \omega_e i_q + L_d \cdot \dfrac{di_d}{dt} \\ u_q = Ri_q + L_d \cdot \omega_e i_d + L_q \cdot \dfrac{di_q}{dt} + \omega_e \psi_f \end{cases} \tag{1}$$

where u_d denote the d-axis voltage, u_q denote the q-axis voltage; i_d denote the d-axis current, i_q denote the q-axis current; R is the stator resistance; ω_e is the electrical angular velocity; ψ_f is the magnetic chain of permanent magnets; L_d denote the d-axis inductance, L_q denote the q-axis inductance, and the values of the d-axis inductance and the q-axis inductance in SPMSM are equal, i.e., $L_d = L_q = L$.

2.2 Conventional T-MPCC Method

As for the T-MPCC method, the control block diagram consists of three main parts: current predictive model, one-step delay compensation and minimum cost function. As shown in Fig.2.

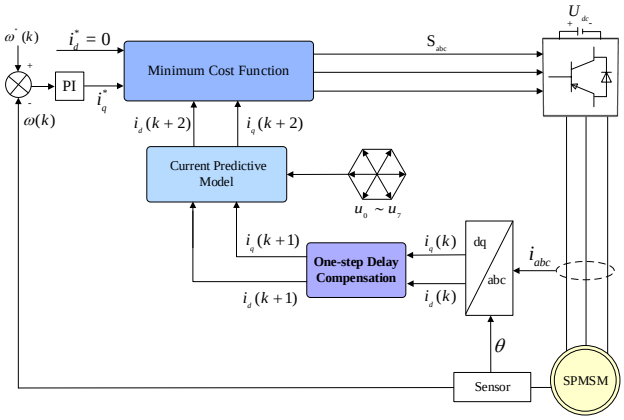

Fig. 2. T-MPCC method control block diagram

From the *d-q*-axis voltage mathematical model, the forward Euler discretization equation is used to predict the *d-q*-axis current at the next moment, and the specific current prediction equation is shown below:

$$\begin{cases} i_d(k+1) = \left(1 - \dfrac{T_s R}{L}\right) \cdot i_d(k) + \dfrac{T_s}{L} \cdot u_d(k) + T_s \omega_e i_q(k) \\ i_q(k+1) = \left(1 - \dfrac{T_s R}{L}\right) \cdot i_q(k) - T_s \omega_e i_d(k) + \dfrac{T_s}{L} \cdot [u_q(k) + \omega_e \psi_f] \end{cases} \tag{2}$$

where T_s is the control period of the drive system.

In real motor control systems, due to hardware and other factors, the control system will have computational delays, so one-step delay compensation is required. After adding one step of delay compensation, the prediction model is updated as:

$$\begin{cases} i_d(k+2) = \left(1 - \dfrac{T_s R}{L}\right) \cdot i_d(k+1) \\ \qquad + T_s \omega_e i_q^p(k+1) + \dfrac{T_s}{L} \cdot u_d(k+1) \\ i_q(k+2) = \left(1 - \dfrac{T_s R}{L}\right) \cdot i_q(k+1) \\ \qquad - T_s \omega_e i_d^p(k+1) + \dfrac{T_s}{L} \cdot [u_q(k+1) + \omega_e \psi_f] \end{cases} \tag{3}$$

The 8 candidate voltage vectors (VVs) are brought into the prediction equation to get 8 predicted currents after delay, which are brought into the minimum cost function to select the optimal voltage vector (VV) and act on the motor through the inverter. The minimum cost function can be expressed as:

$$\mathrm{m} = \left| i_d^{ref} - i_d(k+2) \right| + \left| i_q^{ref} - i_q(k+2) \right| \tag{4}$$

where i_d^{ref} denote the *d*-axis reference value, and i_q^{ref} denote the *q*-axis reference value.

3 Proposed LPM-MPCC Method

In this paper, a low parameter-dependent model control method for PMSM drives is proposed, this method has a low dependence on the model parameters. The control method is suitable for SPMSM, and extracts the parameter values of inductance and magnetic flux by the error values of q-axis prediction currents in the ideal case without parameter perturbation and in the actual working condition. The extracted inductance and flux parameter values are brought into a simplified current prediction model and then adding one-step delay compensation to predicte the next moment current value.. Finally, the reference currents at which the candidate VVs act are calculated by enumeration and the optimal VV is selected by minimum cost function to be acted on the SPMSM motor by the inverter. The control block diagram of the LPM-MPCC control method for SPMSM drives is shown in Fig. 3.

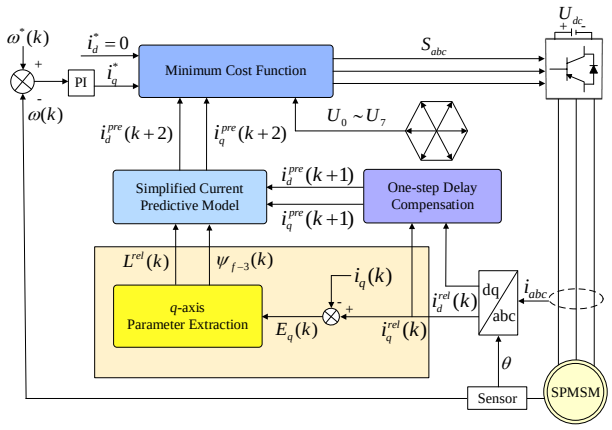

Fig. 3. LPM-MPCC method control block diagram

The relevant literature has demonstrated that resistance parameter mismatch almost has no effect on the control system, whereas inductance and magnetic flux mismatch can lead to a degradation of the overall system performance. Therefore, the focus of this paper is to solve the problem of inductance and magnetic flux parameter mismatch. In Eq. 2, since the value of T_sR/L is much less than 1, the value of $1-T_sR/L$ can be approximated as 1. The simplified current prediction model is Eq. 5:

$$\begin{cases} i_d(k+1) = i_d(k) + T_s\omega_e i_q(k) + \dfrac{T_s}{L(k)}u_d(k) \\ i_q(k+1) = i_q(k) - T_s\omega_e i_d(k) + \dfrac{T_s}{L(k)}[u_d(k) - \omega_e\psi_f(k)] \end{cases} \tag{5}$$

where $\Delta L(k)$ denotes the inductance perturbation error value at the *k* moment, $\Delta\psi_f(k)$ denotes the magnetic flux perturbation error value at the *k* moment.

$$\begin{cases} L^{rel}(k) = L(k) + \Delta L(k) \\ \psi_f^{rel}(k) = \psi_f(k) + \Delta\psi_f(k) \end{cases} \tag{6}$$

The simplified current prediction model containing the actual motor parameters can be expressed as Eq. 7:

$$\begin{cases} i_d^{rel}(k+1) = i_d(k) + T_s\omega_e i_q(k) + \dfrac{T_s}{L^{rel}(k)}\cdot u_d(k) \\ i_q^{rel}(k+1) = i_q(k) - T_s\omega_e i_d(k) + \dfrac{T_s}{L^{rel}(k)}\cdot[u_d(k) - \omega_e\psi_f^{rel}(k)] \end{cases} \tag{7}$$

By using the Euler discretization method to discretize the *q*-axis voltage mathematical equation of the PMSM, the *q*-axis magnetic flux expression can be obtained as follows:

$$\begin{aligned} \psi_f^{rel}(k) = {} & \frac{u_q(k) - Ri_q(k)}{\omega_e} \\ & - L^{rel}(k)\left[\frac{i_q(k) - i_q(k-1)}{T_s\omega_e} - i_d(k)\right] \end{aligned} \tag{8}$$

From the above equation, it is clear that the magnetic flux changes with the change in inductance of the *d*-*q* axis as shown in Eq:

$$\psi_f^{rel}(k) = f\left(L^{rel}(k)\right) \tag{9}$$

In order to facilitate the derivation of the current error equations for the *d*-axis and *q*-axis in the ideal case without parameter perturbation and in the actual working condition, it is assumed that the magnetic flux of the *q*-axis is constant and its error perturbation is small in practice. From the simplified current prediction model, the current errors of *d*-axis and *q*-axis in the two cases are Eq. 10, respectively:

$$\begin{aligned} E_q(k+1) &= i_q^{rel}(k+1) - i_q(k+1) \\ &= \left(D^{rel}(k) - D\right) * \left(u_q(k) - \omega_e\psi_f^{rel}(k)\right) \end{aligned} \tag{10}$$

where $D^{rel}(k)$ denotes the value of T_s/L under the actual working condition, $D^{rel}(k) = T_s/L^{rel}(k)$, D denotes the value of T_s/L under the ideal working condition without parameter perturbation, $D = T_s/L(k)$, and it is worth noting that D is invariant under the ideal condition, so the values of the *k* moment and the *k*-1 moment should be equal.

Based on the above equation, the following expression can be deduced:

$$\begin{aligned} D &= D^{rel}(k) - \frac{E_q(k+1)}{u_q(k) - \omega_e\psi_f^{rel}(k)} \\ &= D^{rel}(k-1) - \frac{E_q(k)}{u_q(k-1) - \omega_e\psi_f^{rel}(k)} \end{aligned} \tag{11}$$

When making a current prediction for the next moment in the current prediction model, the value of $D^{rel}(k)$ in the actual working condition should be the same as the value of D in the ideal case, and thus can be obtained:

$$\begin{aligned} D^{rel}(k) &= D \\ &= D^{rel}(k-1) - \frac{E_{\mathrm{q}}(\mathrm{k})}{u_{\mathrm{q}}(k-1) - \omega_{\mathrm{e}}\psi_f^{rel}(k)} \end{aligned} \tag{12}$$

In order to further improve the accuracy of parameter extraction and suppress harmonic interference, the extracted inductor parameters need to be low-pass filtered.

$$D^{rel}(k) = \mu \cdot D^{rel}(k) + (1-\mu) \cdot D^{rel}(k-1) \tag{13}$$

The coefficient μ of the low-pass filter is set to 0.01 as verified by simulation experiments.

In order to improve the smoothness of the calculated magnetic flux, it is necessary to average the values of magnetic flux at different moments *k*, *k*-1 and *k*-2. According to Eq. 8, an expression for the magnetic flux of the three moments can be obtained as shown in Eq. 14:

$$\begin{cases} \psi_f^{rel}(k) = \dfrac{u_{\mathrm{q}}(k) - Ri_{\mathrm{q}}(k)}{\omega_{\mathrm{e}}} - L^{rel}(k)[\dfrac{i_{\mathrm{q}}(k) - i_{\mathrm{q}}(k-1)}{T_{\mathrm{s}}\omega_{\mathrm{e}}} - i_d(k)] \\ \psi_f^{rel}(k-1) = \dfrac{u_{\mathrm{q}}(k-1) - Ri_{\mathrm{q}}(k-1)}{\omega_{\mathrm{e}}} \\ \qquad -L^{rel}(k-1)[\dfrac{i_{\mathrm{q}}(k-1) - i_{\mathrm{q}}(k-2)}{T_{\mathrm{s}}\omega_{\mathrm{e}}} - i_d(k-1)] \\ \psi_f^{rel}(k-2) = \dfrac{u_{\mathrm{q}}(k-2) - Ri_{\mathrm{q}}(k-2)}{\omega_{\mathrm{e}}} \\ \qquad -L^{rel}(k-2)[\dfrac{i_{\mathrm{q}}(k-2) - i_{\mathrm{q}}(k-3)}{T_{\mathrm{s}}\omega_{\mathrm{e}}} - i_d(k-2)] \end{cases} \tag{14}$$

This is obtained by calculating the average value of the magnetic flux for the current time period and the previous two time periods:

$$\psi_{f-3}(k) = \frac{\psi_f^{rel}(k) + \psi_f^{rel}(k-1) + \psi_f^{rel}(k-2)}{3} \tag{15}$$

The joint equations Eq. 8, Eq. 12 and Eq. 15 can be solved for the actual inductance and magnetic flux parameter values at k moment, thus completing the extraction of the inductance and magnetic flux parameters, and the equations of the joint equations are as follows:

$$\begin{cases} L^{rel}(k) == \dfrac{T_s}{D^{rel}(k-1) - \dfrac{E_{\mathrm{q}}(\mathrm{k})}{u_{\mathrm{q}}(k-1) - \omega_{\mathrm{e}}\psi_f^{rel}(k)}} \\ \psi_f^{rel}(k) = \dfrac{u_{\mathrm{q}}(k) - Ri_{\mathrm{q}}(k)}{\omega_{\mathrm{e}}} \\ \qquad -L^{rel}(k)[\dfrac{i_{\mathrm{q}}(k) - i_{\mathrm{q}}(k-1)}{T_{\mathrm{s}}\omega_{\mathrm{e}}} - i_d(k)] \\ \psi_{f-3}(k) = \dfrac{\psi_f^{rel}(k) + \psi_f^{rel}(k-1) + \psi_f^{rel}(k-2)}{3} \end{cases} \tag{16}$$

The actual inductance and magnetic flux values extracted from the *q*-axis are brought into the simplified *d-q* axis current prediction model:

$$\begin{cases} i_d^{pre}(k+1) = i_d(k) + T_s\omega_e i_q(k) + \dfrac{T_s}{L^{rel}(k)}u_d(k) \\ i_q^{pre}(k+1) = i_q(k) - T_s\omega_e i_d(k) \\ \qquad + \dfrac{T_s}{L^{rel}(k)}[u_q(k) - \omega_e\psi_{f-3}(k)] \end{cases} \tag{17}$$

After adding one step of delay compensation, the current predictive model is updated as:

$$\begin{cases} i_d^{pre}(k+2) = i_d^{pre}(k+1) + T_s\omega_e i_q^{pre}(k+1) \\ \qquad + \dfrac{T_s}{L^{rel}(k+1)}u_d(k+1) \\ i_q^{pre}(k+2) = i_q^{pre}(k+1) - T_s\omega_e i_d^{pre}(k+1) \\ \qquad + \dfrac{T_s}{L^{rel}(k+1)}[u_q(k+1) - \omega_e\psi_{f-3}(k+1)] \end{cases} \tag{18}$$

Finally, the reference currents at which the candidate VVs act are calculated by enumeration, and the optimal VV is selected and acted on the SPMSM by the current error cost function. The current error cost function expression is as follows:

$$m = \left|i_d^{ref} - i_d^{pre}(k+2)\right| + \left|i_q^{ref} - i_q^{pre}(k+2)\right| \tag{19}$$

4 Simulation Experimental Results

In this paper, the control effect of the LPM-MPCC method is verified by the MATLAB/Simulink, and the motor parameters of SPMSM are shown in Table I.

 DOI:10.30420/566414062

TABLE I

Symbol	Value	Symbol	Value
U_{dc} (V)	310	J (kg.m2)	0.00046
R (Ω)	3.18	T_N (N·m)	5
L (mH)	8.5	n_N (r/min)	2000
ψ_f (Wb)	0.325	p	2
P_n(kW)	1.25	I_N (A)	5

In the steady state condition, this paper compares and analyses the LPM-MPCC method with the T-MPCC method, which is convenient to observe the steady-state performance of the LPM-MPCC method. The total harmonic distortion (THD) of the two methods is compared at a control frequency of 10 kHz, and the simulation experimental results are shown in Fig. 4.

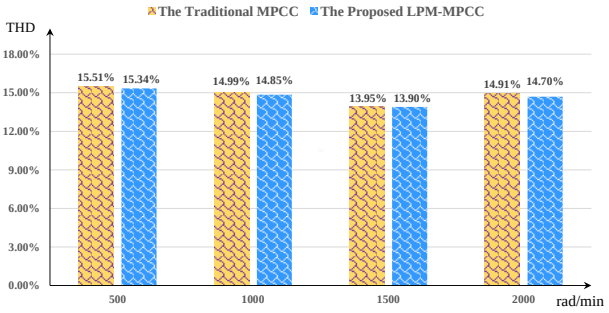

Fig. 4. THD of phase current for conventional MPCC method and LPM-MPCC method

According to Fig. 4, the THD of the LPM-MPCC control method is basically the same as that of the conventional MPCC control method at different speeds. This indicates that the LPM-MPCC method can achieve the same control effect as the T-MPCC method, and the LPM-MPCC method can significantly reduce the dependence of the prediction model on the SPMSM parameters.

Fig. 5 shows the simulation experimental results of the LPM-MPCC method at different speeds, rated load torque.

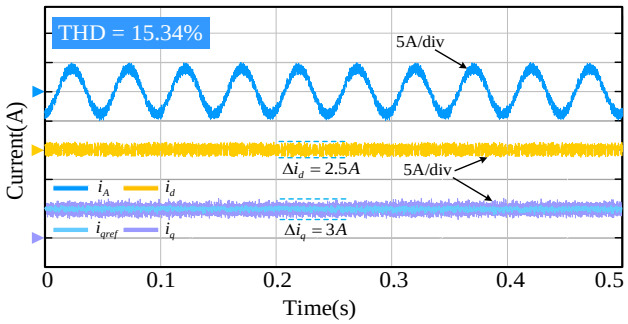

(a)

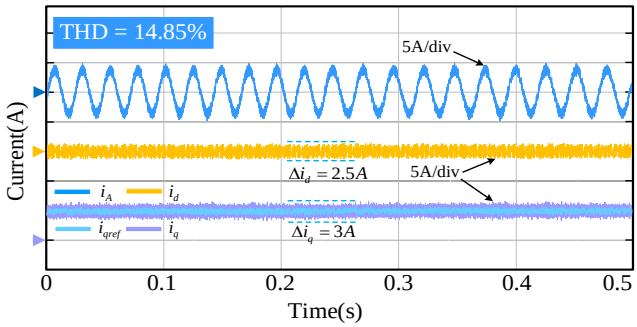

(b)

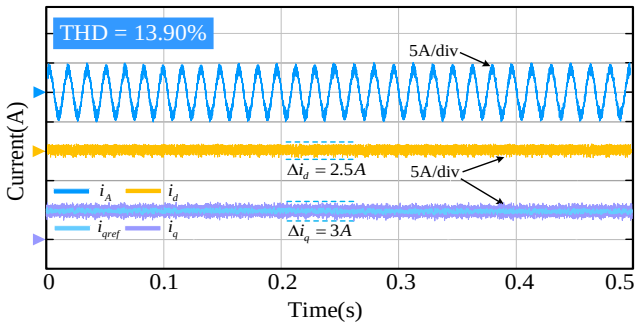

(c)

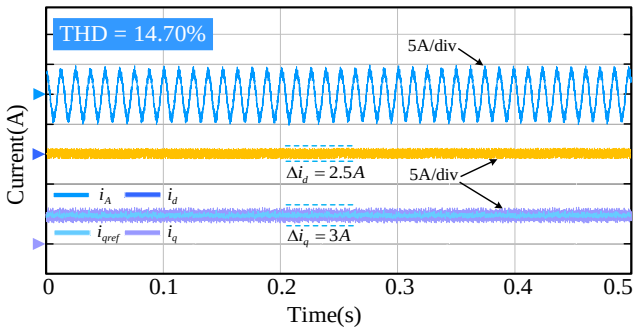

(d)

Fig. 5. Simulation results of LPM-MPCC method: (a) at 500rpm and 5N.m rated load torque (b) at 1000rpm and 5N.m rated load torque (c) at 1500rpm and 5N.m rated load torque (d) at 2000rpm and 5N.m rated load torque.

Fig. 6 gives the simulation results of parameter extraction of the inductor parameters at rated load torque, at different speeds, for the time period from 0.2s to 0.45s for the steady state condition.

ISBN 978-3-8007-6414-3

 DOI:10.30420/566414062

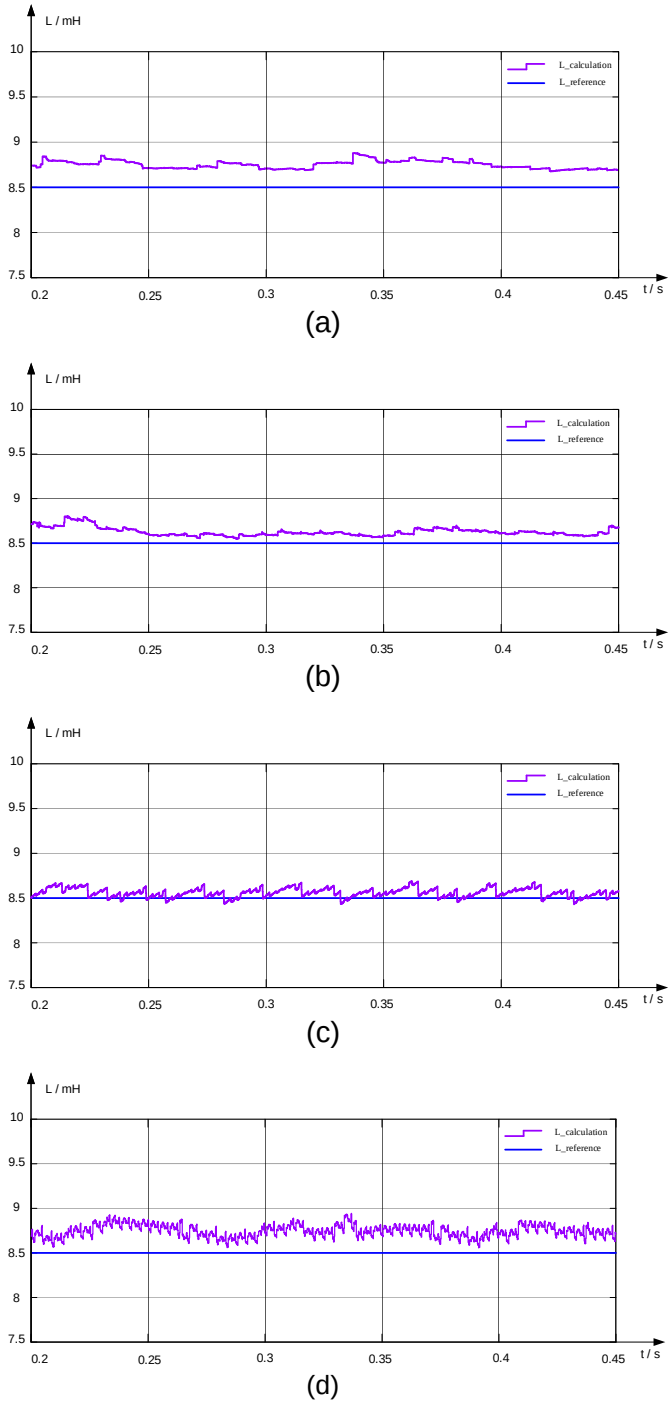

Fig. 6. LPM-MPCC method inductance parameter extraction results: (a) at 500rpm and 5N.m rated load torque (b) at 1000rpm and 5N.m rated load torque (c) at 1500rpm and 5N.m rated load torque (d) at 2000rpm and 5N.m rated load torque.

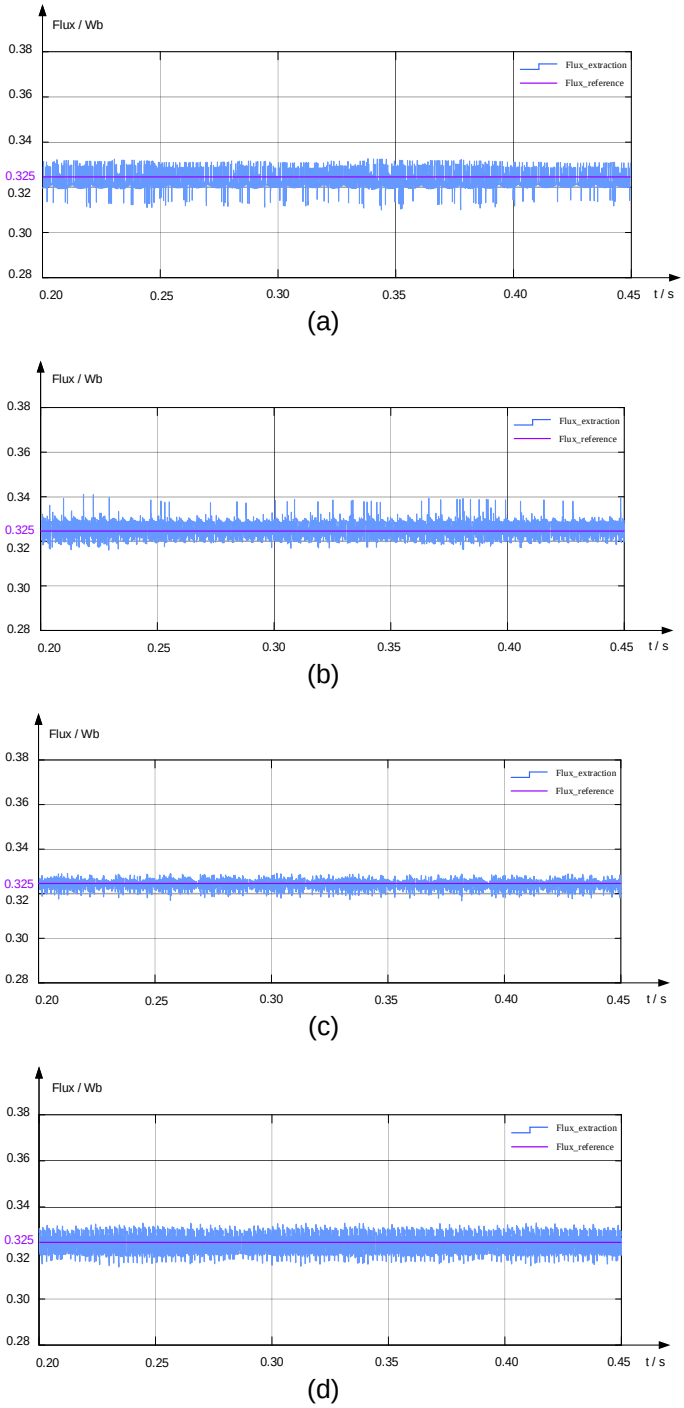

Fig. 7. Magnetic flux parameter extraction results of LPM-MPCC method: (a) at 500rpm and 5N.m rated load torque (b) at 1000rpm and 5N.m rated load torque (c) at 1500rpm and 5N.m rated load torque (d) at 2000rpm and 5N.m rated load torque.

Fig. 7 gives the parameter extraction results of the magnetic flux parameter for the time period from 0.2s to 0.45s for the steady state case at the rated load torque, and at different rotational speeds.

5 Conclusion

Aiming at the unfavorable effects brought by the perturbation errors of motor parameters, this paper proposes and verifies the effectiveness of the LPM-MPCC method. The motor parameters are extracted

ISBN 978-3-8007-6414-3

by the current errors of *q*-axis under ideal and actual working conditions, and then the extracted motor parameters are brought into the simplified current prediction model for real-time updating prediction, which makes the current prediction model more accurate and enhances the parameter robustness of the drive control system. In addition, not only does LPM-MPCC method can accurately extract the inductance and magnetic flux parameter of the SPMSM at different moments, but also the control effect is very close to the conventional MPCC method.

6 References

[1] Z. Chen, T. Shi, Z. Lin, Z. Wang, and X. Gu, “Analysis and control of current harmonic in IPMSM field-oriented control system,” IEEE Trans. Power Electron., vol. 37, no. 8, pp. 9571–9585, Aug. 2022.

[2] F. Niu, K. Li, and Y. Wang, “Direct torque control for permanent-magnet synchronous machines based on duty ratio modulation,” IEEE Trans. Ind. Electron., vol. 62, no. 10, pp. 6160–6170, Oct. 2015.

[3] X. Zhang, H. Bai, and M. Cheng, “Improved model predictive current control with series structure for PMSM drives,” IEEE Trans. Ind. Electron, vol. 69, no. 12, pp. 12437–12446, Dec. 2022.

[4] J. Wang, H. Yang, Y. Liu and J. Rodríguez, "Low-Cost Multistep FCS-MPCC for PMSM Drives Using a DC Link Single Current Sensor," in IEEE Transactions on Power Electronics, vol. 37, no. 9, pp. 11034-11044, Sept. 2022.

[5] X. Zhang, C. Zhang, Z. Wang and J. Rodríguez, "Motor-Parameter-Free Model Predictive Current Control for PMSM Drives," in IEEE Transactions on Industrial Electronics, vol. 71, no. 6, pp. 5443-5452, Jun. 2024.

[6] X. Zhang and Z. Wang, "Simple Robust Model Predictive Current Control for PMSM Drives Without Flux-Linkage Parameter," in IEEE Transactions on Industrial Electronics, vol. 70, no. 4, pp. 3515-3524, Apr. 2023.

[7] X. Zhang, B. Hou, and Y. Mei, “Deadbeat predictive current control of permanent-magnet synchronous motors with stator current and disturbance observer,” IEEE Trans. Power Electron., vol. 32, no. 5, pp. 3818–3834, May 2017.

[8] Z. Zhang, Y. Liu, X. Liang, H. Guo, and X. Zhuang, “robust model predictive current control of PMSM based on nonlinear extended state observer,” IEEE J. Emerg. Sel. Topics Power Electron., vol. 11, no. 1, pp. 862–873, Feb. 2023.

[9] X. Zhang, L. Zhang, and Y. Zhang, “Model predictive current control for PMSM drives with parameter robustness improvement,” IEEE Trans. Power Electron., vol. 34, no. 2, pp. 1645–1657, Feb. 2019.

[10] T. Wang, Y. Hu, Z. Wu, and K. Ni, “Low-switching-loss finite control set model predictive current control for IMs considering rotor related inductance mismatch,” IEEE Access, vol. 8, pp. 108928–108941, 2020.

[11] G. Gatto, I. Marongiu, and A. Serpi, “Discrete-time parameter identification of a surface-mounted permanent magnet synchronous machine,” IEEE Trans. Ind. Electron., vol. 60, no. 11, pp. 4869–4880, Nov. 2013.

[12] Y. Shi, K. Sun, L. Huang and Y. Li, "Online Identification of Permanent Magnet Flux Based on Extended Kalman Filter for IPMSM Drive With Position Sensorless Control," in IEEE Transactions on Industrial Electronics, vol. 59, no. 11, pp. 4169-4178, Nov. 2012.

[13] D. Q. Dang, M. S. Rafaq, H. H. Choi and J. -W. Jung, "Online Parameter Estimation Technique for Adaptive Control Applications of Interior PM Synchronous Motor Drives," in IEEE Transactions on Industrial Electronics, vol. 63, no. 3, pp. 1438-1449, Mar. 2016.